Determinants of SARS-CoV-2 transmission to guide vaccination strategy in an urban area

Sarah C. Brüningk[1,2,*], Juliane Klatt[1,2,*], Madlen Stange[2,3,5,*], Alfredo Mari[2,3,5], Myrta Brunner[3,4], Tim-Christoph Roloff[2,3,5], Helena M.B. Seth-Smith[2,3,5], Michael Schweitzer[3,5], Karoline Leuzinger[6,15], Kirstine K. Søgaard[3,5], Diana Albertos Torres[3,5], Alexander Gensch[3], Ann-Kathrin Schlotterbeck[3], Christian H. Nickel[7], Nicole Ritz[9], Ulrich Heininger[9], Julia Bielicki[9], Katharina Rentsch[10], Simon Fuchs[12], Roland Bingisser[7], Martin Siegemund[11], Hans Pargger[11], Diana Ciardo[13], Olivier Dubuis[13], Andreas Buser[14], Sarah Tschudin-Sutter[8], Manuel Battegay[8], Rita Schneider-Sliwa[4], Karsten M. Borgwardt[1,2,+], Hans H. Hirsch[6,8,15,+], Adrian Egli[3,5,+,†]

[1]*Machine Learning & Computational Biology, Department of Biosystems Science and Engineering, ETH Zurich, Basel, Switzerland*

[2]*Swiss Institute for Bioinformatics (SIB), Lausanne, Switzerland*

[3]*Applied Microbiology Research, Department of Biomedicine, University of Basel, Basel, Switzerland*

[4]*Human Geography, Department of Environmental Sciences, University of Basel, Basel, Switzerland*

[5]*Clinical Bacteriology and Mycology, University Hospital Basel & University of Basel, Basel, Switzerland*

[6]*Clinical Virology, University Hospital Basel & University of Basel, Basel, Switzerland*

[7]*Emergency Department, University Hospital Basel, Basel, Switzerland*

[8]*Infectious Diseases and Hospital Epidemiology, University Hospital Basel & University of Basel,*

Basel, Switzerland

[9] *Paediatric Infectious Diseases and Vaccinology, University of Basel Children's Hospital Basel and University of Basel, Basel, Switzerland*

[10] *Laboratory Medicine, University Hospital Basel, Basel, Switzerland*

[11] *Intensive Care Medicine, University Hospital Basel, Basel, Switzerland*

[12] *Health Services for the Basel-City, Basel, Switzerland*

[13] *Viollier AG, Allschwil, Switzerland*

[14] *Regional Blood Transfusion Service, Swiss Red Cross, Basel, Switzerland*

[15] *Transplantation & Clinical Virology, Department Biomedicine, University of Basel, Basel, Switzerland*

**These authors contributed equally to this work*

+These authors share senior authorship

†*corresponding author*

Supplementary Material

Supplementary Methods

PCR testing and whole-genome sequencing. PCR testing was available rapidly and frequent testing was established and supported by local guidelines by the end of February 2020, before the first case arrived[1]. SARS-CoV-2 testing was made available (i) via a walk-in test center in

the city center affiliated to the University Hospital Basel, which allowed screening of legal-aged patients with mild and severe symptoms, (ii) via the University Children's Hospital for minors on recommendation by the pediatricians, and (iii) via the obligatory screening of any incoming patients to the University Hospital Basel irrespective of symptoms. Testing in case of symptoms was covered by the Swiss mandatory health insurance scheme preventing sampling bias from affluent socioeconomic population groups. In total 7073 PCR tests from Basel-City residents were performed at the University Hospital Basel (UHB) (750 of which were SARS-CoV-2 positive) dating between 25^{th} of February and 22^{nd} of April, 2020. The total number of positive cases for Basel-City including also external testing sources for the same time range was 928, hence the cases registered at the UHB cover 80.8% of the total case burden[2]. The ratio of negative to positive PCR tests changed during the local epidemic with a median of 10.6% positive PCR tests (Figure 2B). We successfully sequenced SARS-CoV-2 whole genomes from 411 unique patients (54.8% of our cases, 44% of all cases). Of these, 247 (247/411, 60%) could be attributed to contain the C15324T mutation in the B.1 lineage (and therefore called B.1-C15324T) characteristic to the virus variant that originated in this tri-national area[3].

Geographic mapping and socioeconomic stratification. Basel-City is divided into 21 urban quarters and had a population of 201,971 in 2020[4] (Figure S9). For subsequent analyses, a total of 1,078 statistical (housing) blocks (a city block partitioned by e.g. streets, rivers) were identified within the city quarters. Each individual PCR test (N = 7073), irrespective of the result, was linked to the patient's place of residence anonymized at the scale of statistical blocks in

ArcMap 10.7 (by ESRI). To explore the statistical association between SARS-CoV-2 transmission and socioeconomic factors, we employed data provided by the Canton of Basel-City's office for statistics for the year of 2017 (most recent data available), that specified the values for various socioeconomic indicators for each statistical block (except for those blocks where privacy legislation did not permit the sharing of such information). The indicators under study were (i) the living space (per capita in m^2), (ii) the share of 1-person private households, (iii) the median income (CHF), and (iv) the population seniority (percentage of senior citizens aged over 64 years per block). According to these socioeconomic indicators, blocks were allocated to one of three socioeconomic city tertiles (T1:≤33rd percentile , T2: 33rd to 66th percentile T3:>66th percentile) where possible (e.g. Figure 3A). In general, sparsely populated blocks displayed a maximum of three positive cases and had to be excluded from analysis. All following analyses with respect to socioeconomic factors were based on these city partitions.

Phylogenetic inference and cluster analysis. Whole-SARS-CoV-2-genomes from Basel-City patients were assembled using our custom analysis pipeline COVGAP[3] (github.com/appliedmicrobiologyresea CoV-2/). Global sequences and metadata were downloaded from GISAID[5,6] (as of October 22,2020; 155,278 consensus sequences). Sequences with more than 10 percent N's (27,013) and with incomplete dates (43,466) were removed. 84,799 sequences remained which were joined with Basel genomes. Filtering for the period of interest until April 22^{nd} retained 39,913 genomes, of which 411 are from Basel-City residents dating from February 26^{th} (first case) to April 22^{nd}, 2020.

To infer relatedness among the viral genomes and spread of SARS-CoV-2 in Basel-City, a time-calibrated phylogeny that was rooted to the first cases in Wuhan, China from December 2019, was inferred using a subset of the global genomes. For subsetting, we included 30 genomes per country and month, whereby all genomes from Basel-City were retained, totalling 3,495 genomes, using the nextstrain software v.2.0.0 (nextstrain.org) and augur v.8.0.0[7] as described in detail in [3].

The resulting global phylogeny was used to infer phylogenetic clusters in Basel-City. First, polytomies, which are caused by identical genomes in the tree were resolved using ETE3 v.3.1.1[8]. Cluster Picker v.1.2.3 [9] was then used to identify clusters in the resolved tree (options 0, 0, 4e-4, 5). Identified clusters were consolidated with epidemiological data (occupation in a health service job, resident of a care home, contact to positive cases, onset of symptoms, place of infection) to confirm the suitability of the divergence parameter. Cluster Matcher v.1.2.4[9] was then used to combine ancillary geographic (quarter), and socioeconomic or demographic information that were subdivided into tertiles on identified clusters.

To test whether related genomes in Basel-City cluster according to a) quarter, b) living space per person, c) share of 1-person households, d) median income, or e) seniority a custom python-script for a random permutation test was performed[10] (github.com/appliedmicrobiologyresearch/Influenza-2016-2017). The results for clustering within and among urban quarter and tertiles in socioeconomic determinants were visualized using circos v.0.69[11].

Serology. SARS-CoV-2 antibody responses were determined in a total of 2,019 serum samples collected from individuals between 25^{th} of February and 22^{nd} of May, 2020, to account for seroconversion. Serology information was used to estimate the fraction of unreported cases as follows: An estimated 1.88% (38/2,019) of the Basel-City population was infected with SARS-CoV-2. Of these 60% would be attributed to the B.1-C15324T variant, leading to a percentage of 88% of unreported/unsequenced cases to consider.

Mobility data. We employed the official traffic model provided by the traffic department of Basel-City [12]. The latter consists of the 2016 average A-to-B traffic on a grid of ~1400 counting zones for four transport modalities: foot, bike, public motorized transport and private motorized transport. We further obtained weekly averages of pass-by traffic for the same count zones over the period of the first wave of the pandemic for the categories of combined foot and bike traffic, as well as private motorized traffic. Additionally, weekly public-transport passenger loads were provided by both the Swiss Federal Rail Company and the local public transport services. From these datasets, we computed the spatio-temporal variation of mobility within the city as follows. Spatial variation was obtained by aggregating A-to-B traffic between the aforementioned counting zones, first to the statistical block level (by identifying the nearest housing block with respect to a zone's centroid), and second to tertile level via a statistical-block's association with a socioeconomic indicator tertile. This resulted in a there-by-three mobility matrix M_{jk} whose diagonal entries represent within-tertile mobility, while off-diagonal entries represent inter-tertile mobility. This matrix was normalized to one since only relative

differences were relevant in our model. We hence obtained a direct link between mobility and socioeconomic/demographic information agglomerated based on the unifying scale of statistical blocks. Temporal variation was obtained by computing the weighted sum of the private transport time-series provided by the traffic department and the public transport time-series provided the Swiss Federal Rail Company and the local public transport services. This sum was then normalized and smoothed with a uni-variate spline resulting the final time-series for temporal mobility variation employed in our model (denoted as $\alpha_{mob}(t)$), see Figure 3D).

Dynamic changes in social interaction. SARS-CoV-2 transmission is contact-based. While the number of contacts potentially taking place within a day and a city is largely influenced by human mobility as estimated above, the risk of a contact becoming a transmission event is further determined by the precautions taken by the two individuals being in contact (such as washing hands, wearing masks, distance keeping). Both aspects together–mobility and risk-mitigating social behaviour within a (sub-)population–eventually result in an effective, time-dependent, reproductive number characterizing the virus's transmission within that (sub-)population. Hence, there are three relevant time-series: changes in the overall effective reproductive number, in mobility, and in social behaviour. While the computation of the temporal variations in mobility was described above, the time-dependent effective reproductive number is obtained by applying a Kalman filter [13,14] to the piece-wise linearised time-series of daily confirmed cases of individuals having contracted the B.1-C15324T variant of SARS-CoV-2. Assuming a multiplicative model, the time-dependence of residual transmission risk stemming from lack of

precaution in social interaction (denoted as $\alpha_{soc}(t)$), is obtained by point-wise division of the time-dependence of the effective reproductive number by the mobility time-series (depicted in Figure 3D). Thus we are adhering to the logic that in the extreme case of zero mobility, no transmission can take place despite a finite risk of transmission rooted in a lack of precautions, while on the other hand in the case of zero risk of transmission due to perfect precautions, no transmission can take place despite non-zero mobility. Such logic dictates the choice of a multiplicative rather than additive model.

Fitting procedure and evaluation of the SEIR-model. In total 247 cases within the time period from the 25th of February until the 22nd of April were included in this analysis. For all data a seven day moving window average was taken to account for reporting bias on weekends, and cumulative numbers of infected cases (compartment I) were calculated. Due to the loss of single sequencing plate, missing numbers on the 29th, 30th and 31st of March were imputed by assuming a constant ratio of the B.1-C15324T variant amongst the sequenced samples. Simulations were initialized on the 22nd of February, the estimated date of the occurrence of the initial exposed cases[3].

The ODE system was implemented in python (version 3.8.) using the scipy functions *odeint* to iteratively solve the system of equations and *minimize* (with L-BFGS algorithm, cut-off tolerance of 10^{-7}) for parameter fitting based on the average sum of squared differences between the logarithm of estimated and recorded cases. Points with cumulative case numbers below 15 were not scored in the cost-function since the continuum assumption of the model may not

be satisfied for small case numbers. The fit was performed simultaneously for all four socioeconomic partitions to account for the shared parameters T_{infU} (obtained 1.8 days) and T_{infP} (obtained 2.1 days). Fit performance was evaluated based on root mean squared error (RMSE) between predicted and recorded case numbers. Data uncertainty and the corresponding influence on parameter estimation were assessed by bootstrapping. For each of 50 bootstraps each data point was randomly shifted according to numbers drawn from a normal distribution centered around zero and standard deviation 0.3. Results are shown as mean values over bootstraps and bootstrap uncertainty bands.

Scenario simulation. The impact of mobility relative to social interaction was analysed by recalculating the predicted epidemic trajectory under the constraint of constant intra-urban mobility ($\alpha_{mob}(t) = 1$, scenario M1) or fully restricted ($\alpha_{mob}(t) = 0$, scenario M2) mobility, corresponding to perfect isolation of the affected city areas. These scenarios were compared to the baseline of the actual reduction in mobility (scenario M0).

Vaccination scenarios were simulated as for both 90% and 70% effective vaccines to prevent COVID-19 resembling current vaccine candidate data [15,16], as well as a range of vaccine efficacies to prevent SARS-CoV-2 transmission (60%, 90%). This was achieved by moving the fraction of the vaccinated and not transmitting population from the susceptible to the recovered compartment U_r and calculating the spread of the pandemic with constant effective reproductive number and intra-city mobility. We accounted for a change in social interaction behaviour following vaccination by assigning a mean social interaction score of the vaccinated and not-

vaccinated population amongst the initial susceptibles ($\alpha_{soc,vacc}(t) = 0.75$, $\alpha_{soc,novacc}(t) = 0.5$). Mobility was modelled as 100% ($\alpha_{mob}(t) = 1$). Two scenarios were investigated and compared to the no vaccine scenario (V0): i) vaccination of a fixed population fraction (one or two thirds) randomly throughout the population (scenario V1), ii) vaccination of the corresponding number of individuals from different socioeconomic groups (scenario V2 (exclusively from T1 median income), V3 (exclusively from T3 seniority), V4 (50% from T1 median income, 50% from T3 seniority)). In order gauge the benefit of a particular vaccination scenario, we calculated the time to reach 50% of intensive care unit (ICU) capacity. The University Hospital Basel has a total of 44 ICU beds. During the first wave, 4.5% of reported SARS-CoV-2 positive cases were admitted to ICU, and their median length of ICU stay was 5.9 days (IQR, 1.5-12.9). If considering additional unreported cases (captured by serological testing), the percentage of patients requiring ICU admission was 1%. Of all SARS-CoV-2 patients with ICU stay, 40% were younger than 64 years resulting in a probability of an under 64 year old infected case to be admitted to ICU of 0.5%. In case of vaccinated populations not at random, we adjust the relevant fraction of ICU cases based on the represented proportions of geq and < population fractions within all susceptibles.

* Relevance of Basel-City in a European context - an overview. Basel-City has to be seen in its larger context: Basel-City is the core city of the trinational Greater Basel area and functional urban area (FUA), according to the official European statistics system. Basel-City is also part of a European cross-border region in the European Employment Services Network (EURES) that promotes labor mobility across state borders and it is a main center in the context of "European

Regions". "European regions" are "designer regions" or spaces of cooperation within well defied action perimeters. The role of such forms of regional governance is to foster cross-border cooperation, regional competitiveness with collaborative development plans in interlinked, interlocking metropolitan regions, which may be organized as "Eurodistricts" and are a mean in the EU-strategy to re-scale and decentralize development through regional institution building. Planning a the Eurodistrict level is regulated by state treaties and can act with a relatively high degree of autonomy from their national governments, mostly in the areas of spatial planning, traffic development and other aspects where links in development are missing.

Moreover, Basel and the Greater Basel area are also part of the Upper Rhine Region Metropolitan Economy, which by regional gross domestic product (GDP) is the eighth largest metropolitan economy in the EU. In summary, the case study of Basel-City is representative or transferable to other similar urban contexts because in the European harmonised statistical classifications (Eurostat and OECD classifications) as a metropolitan area, a functional urban area, and a part of a European cross-border region, it is representative for other urban areas classified similarly. This makes information obtained from analyses of Basel-City comparable and transferable to other such urban areas. This is explained in more detail below.

Basel Metropolitan area: The Greater Basel area is a metropolitan area according the OECD/Eurostat definition, stretching into three countries with a population of around 830,000 in the Trinational Eurodistrict of Basel, an organization of municipalities and cities in the trinational surroundings of Basel and central cooperation body in the agglomeration of Basel [17,18]. Metropolitan regions are NUTS 3 Eurostat statistical subdivisions according to the nomenclature des unités ter-

ritoriales statistiques - a classification of territorial units for statistical analyses. The NUTS classification provides for a harmonised hierarchy of regions and Eurostat lists 541 such metropolitan areas [19].

Metropolitan areas are engines for growth and employment, the centers of competitiveness, and innovation, and contribute strongly to economic growth, social and political functions and are important for local, regional and international transport. Although only Basel-City, or rather, a small number of city quarters were examined here, Basel-City is a "hub", i.e. the core of a larger metropolitan region with a commuter catchment area and on a scale that corresponds to the definitions of OECD and Eurostat (European Statistical Office) which also apply to Switzerland. As such, it is the contextualization of the city/urban quarter study within the larger urban/metropolitan/functional urban area, that make the study area comparable with other such metropolitan regions. Using Basel-City as a case study of an urban core or "core city" of its larger urban area / metropolitan area/ functional urban area makes the city, the study area and the results comparable or transferable to other urban areas/metropolitan areas/ functional urban areas and their core cities.

Basel as a hub of a Functional Urban Area: The Greater Basel area is also a functional urban area (FUA) in the official European statistics system. Functional urban areas consist of a densely inhabited city and a less densely populated commuting zone whose labor market is highly integrated with the city. FUAs extend beyond formal administrative boundaries. The OECD, in cooperation with the EU, has developed a harmonised definition of functional urban

areas (FUAs). Being composed of a city (or core) and its commuting zone, FUAs encompass the economic and functional extent of cities based on daily people's movements [20]. The definition of FUA aims at providing a functional/economic definition of cities and their area of influence, by maximising international comparability and overcoming the limitation of using purely administrative approaches. At the same time, the concept of FUA, unlike other approaches, ensures a minimum link to the government level of the city or metropolitan area. The new harmonized OECD definition of cities, urban areas, functional urban areas and commuting zones allows for the first time a comparison within the European urban hierarchy. It identified 828 (greater) cities with an urban center of at least 50 000 inhabitants in the EU, and the "greater city level" greatly improved international comparability [20].

Basel-City as part of a European EURES-labor market and labor mobility region: Basel-City is also part of a European cross-border region within the European commission's Strategy of Employment, Social Affairs and Inclusion European Employment Services-EURES cooperation network that promotes labor mobility in the EU and its partner countries in terms of assistance for recruitment and job placements, and providing information to cross order workers and employers on issues such as social security, insurance and taxation [21]. EURES is based on technical standards and formats required for a uniform system to enable matching of job vacancies with job applications (Commission Implementing Decision (EU) 2017/1257 of 11 July 2017). EU internal border regions cover 40% of EU territory and are home to almost 2 million cross-border commuters. In 2018, more than 1.5 million people in the EU lived in one country and worked

in another. In the trinational Basel urban area 60,000 persons commute on a daily basis across state borders, of which around 34,000 commute daily into Basel-City[22]. Just as mobility is an important factor in the economy, it may be a driving factor in the transmission of disease which is why the Basel study may be relevant for other cross-border regions in Europe.

Basel-City as part of a European cross-border region: The trinational Basel metropolitan area with Basel-City as its center has been the first to organize itself in private initiative as a "European cross-border region" in 1960 (Regio Basiliensis e.V.) for the purpose of advancing common interests and developments, enhancing cooperation between regions along state borders and between border regions throughout Europe. It has also served as a model for the institutionalised EU cross-border policy by means of INTERREG funding programs that aimed at promoting decentralized regional development through new forms of governance. Cross-border regions have flourished since the 1990 in particular because of their increasingly relevant role as implementation units for European regional policy in a context of multi-level governance [23]. Today, there are some larger 100 cross-border regions as outlined in figure S1. Within the nested hierarchy of European "designer regions" for the purpose of fostering regional development some contain the aforementioned Eurodistricts, which are a rather new model of regional governance for promoting economic development in several contiguous metropolitan areas.

Perimeter of Unified Action of European regional governance: The Greater Basel area is

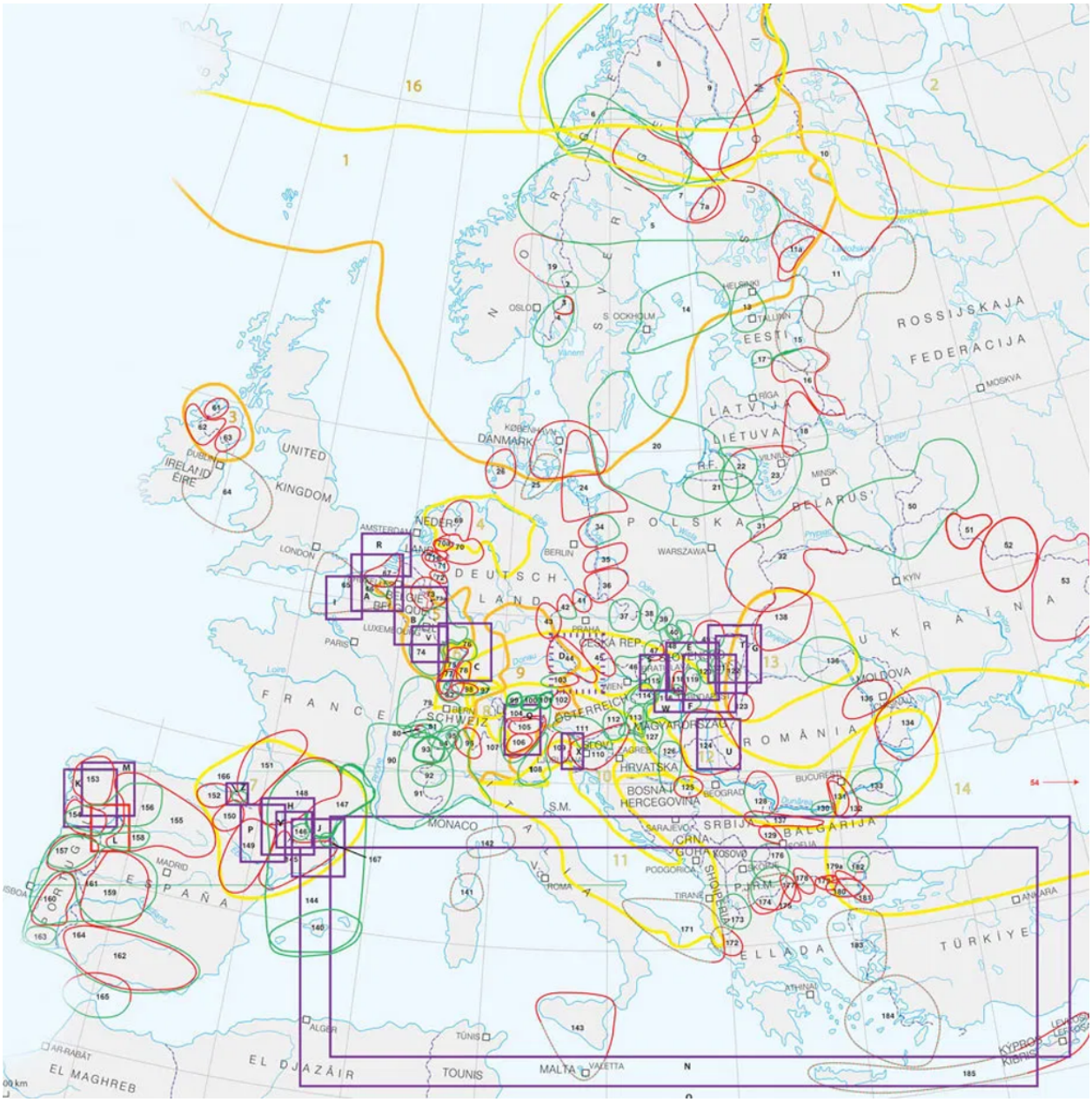

Figure S1: Association of European Border Regions (AEBR) and cross-border cooperation in Europe as shown in [24].

furthermore part of the “Trinational Metropolitan Upper Rhine region” (TMUR). This refers to an innovative governance model for the four sub-areas Alsace, France, Northwest Switzerland, Southern Palatinate and Baden, Germany which together form an internationally strong business and knowledge location. The TMUR region refers to a perimeter of unified planning policy measures within a closely interlinked cross-border territory on issues of common interest. As a rather new form of territorial governance the TMUR region acts as umbrella over the existing metropolitan regions and trinational cooperations in the Upper Rhine and aims to strengthen their competitiveness within Europe and the world, and its public positions with respect to the political centers of Berlin, Paris, Bern, and Brussels. Collaborative efforts are focused on the areas of science, the economy, politics and civil society. By regional GDP and population size the TMUR can be an be seen as a major European metropolitan economy.

Metropolitan areas and metropolitan economies are engines and centers of growth and employment, and their many universities and knowledge institutions are drivers of innovation and international competitiveness. Large urban agglomerations typically combine economic, social and political functions and form important hubs for regional and international connection. Conceptually and methodically it is difficult to view this only in terms of administrative boundaries. The view on large metropolitan areas and regional governance models which encompass multitudes of cities and towns is applied for international comparisons, and in today’s global world the formation of larger metropolitan area governance forms which joins together urbanized areas even across administrative or state borders is the mechanism to achieve joint economic growth. The trinational metropolitan region Upper Rhine, in turn, is a major urban

304 economy within Europe, ranking eighth in terms of regional GDP behind metropolitan areas
305 outlined in Table S1.

Table S1: Selection of European metropolitan areas with GDP, population and GRP. Data obtained from [25–28]

	GRP [bio. euros]	Population [mio.]	GRP per inhabitant
Greater London area	946	19.53	48.443
Paris (Ile de France)	709	12.15	58.358
Rhine-Ruhr area	403	9.63	41.850
Randstadt Netherlands	397	8.15	48.659
Milan (Lombardy)	381	10.02	38.023
Brussels-Antwerp	264	5.67	46.656
Barcelona (Catalonia)	224	7.44	30.101
Trinantional Upper Rhine Metroplitan area	**209**	**5.9**	**34.889**
Frankfurt (Darmstadt)	200	3.95	50.666
Copenhagen-Malmö	180	3.29	54.827
Munich	177	6.12	79.690
Berlin	169	3.65	40.104

* Reasoning for the study design Patterns of SARS-CoV-2 transmission have previously been discussed from different angles either via network and transmission modelling [29], by statistical evaluation [30], or by phylogenetic clustering based on genomic sequencing data[31]. Whereas modelling approaches can account for and simulate rich detail such as socioeconomic and demographic information, it is essential to balance the trade-off between detail described and the number of data points available. Moreover, a more diverse socioeconomic and demographic population structure may make it easier to detect general trends. In order to address these needs, many modelling studies rely on publicly available case numbers without being able to relate the cases to specific socioeconomic parameters and specific geographic locations , or have to perform analysis predominantly for large metropolis. For such scenarios, it is inherently difficult to distinguish the spread of competing viral variants within the same population and to account for new introductions in a model - classical ODE or agent-based models are relying on the assumption of uninterrupted transmission chains, information that whole-genome sequencing can provide. Yet given the cost of such analyses, whole genome sequencing covering entire epidemic waves is often infeasible. In this study we address the aforementioned limitations and choose a trade-off between the population detail studies in-light of limited case numbers for which we hold detailed information, including whole genome sequencing: we perform an analysis for a medium-sized, European city to account for the under-representation of these urban areas in previous modelling approaches. The case data used in this analysis was available for 80% of all reported cases in Basel-City and includes detailed, highly sensitive information on the infected individuals to enable tracing of transmission chains which are not

publicly available. Sequencing was attempted for all samples and based on this data we restricted our analysis to inherently related cases of the B.1-C15324T variant. Although reducing the number of cases to <300, this implies that ODE based models are well suited to describe the dynamic development of these cases. We deliberately choose a continuum approach to incorporate socioeconomic, demographic and mobility information into this compartmental model since more complex network approaches would be infeasible for the final number of cases. This model enables us to evaluate general trends of transmission, such as effective reproductive numbers, and to use this information for vaccine scenario building.

In order to complement this more general analysis, we employ phylogenetic analysis to directly trace transmission clusters in detail. Phylogenetic analysis of positive cases provides rich information on relatedness of cases and hence supports modelling approaches by discerning introduction events and community spread. In this study we combine phylogenetic clustering with mathematical modelling of the SARS-CoV-2 transmission pattern. Our analysis is unique in the way that it is based on a large number of sequenced and phylogenetically related cases (411 sequenced out 750 positives, 247 that belong to a single genomic variant). As such, we however hold rich information for a comparably small, yet densely sampled cohort of cases, and are able to provide a complete picture of SARS-CoV-2 transmission in a medium-sized city by choosing two complementary analysis tools.

* References

A

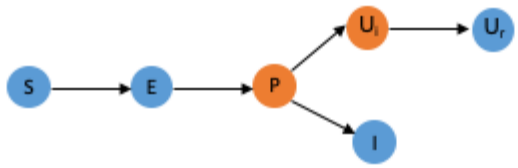

B

$$\frac{dS_j}{dt} = -R_j \alpha_{soc}(t) \alpha_{mob}(t) \frac{S_j}{N_j} \cdot \left[\sum_{k=1}^{3} M_{j,k} \cdot \left(\frac{P_k}{T_{\text{infP}}} + \frac{U_k}{T_{\text{infU}}} \right) \right] \quad (1)$$

$$\frac{dE_j}{dt} = R_j \alpha_{soc}(t) \alpha_{mob}(t) \frac{S_j}{N_j} \cdot \left[\sum_{k=1}^{3} M_{j,k} \cdot \left(\frac{P_k}{T_{\text{infP}}} + \frac{U_k}{T_{\text{infU}}} \right) \right] - \frac{E_j}{T_{\text{inc}}} \quad (2)$$

$$\frac{dP_j}{dt} = \frac{E_j}{T_{\text{inc}}} - \frac{P_j}{T_{\text{infP}}} \quad (3)$$

$$\frac{dI_j}{dt} = (1 - p_{sq}) \frac{P_j}{T_{\text{infP}}} \quad (4)$$

$$\frac{dUi_j}{dt} = p_{sq} \frac{P_j}{T_{\text{infP}}} - \frac{I_j}{T_{\text{infU}}} \quad (5)$$

$$\frac{dUr_j}{dt} = \frac{I_j}{T_{\text{infU}}} \quad (6)$$

Figure S2: Overview of the SEIR model. A: Conceptual overview. We accounted for susceptibles (S), exposed (E, incubation time T_{inc}), and pre-symptomatic yet infectious cases (P). After a presymptomatic time T_{infP}, cases were separated according to the estimated proportion of reported and sequenced cases, p_{sq}, into either reported infectious (I), or unreported infectious (U_i, reproductive number R). Since our data did not include information on recovered patients, a 'recovered' compartment was not included following I. It was assumed that reported cases remained isolated. The unreported compartment transitions to recovery (U_r) after an infectious time T_{infU}. B: Relevant model equations to incorporate connectivity and exchange between the defined tertiles (index j). Cross contamination was included through the mobility matrix M_{jk} and relevant temporal variation of mobility and social interaction (weighting factors $\alpha_{mob}(t)$ and $\alpha_{soc}(t)$).

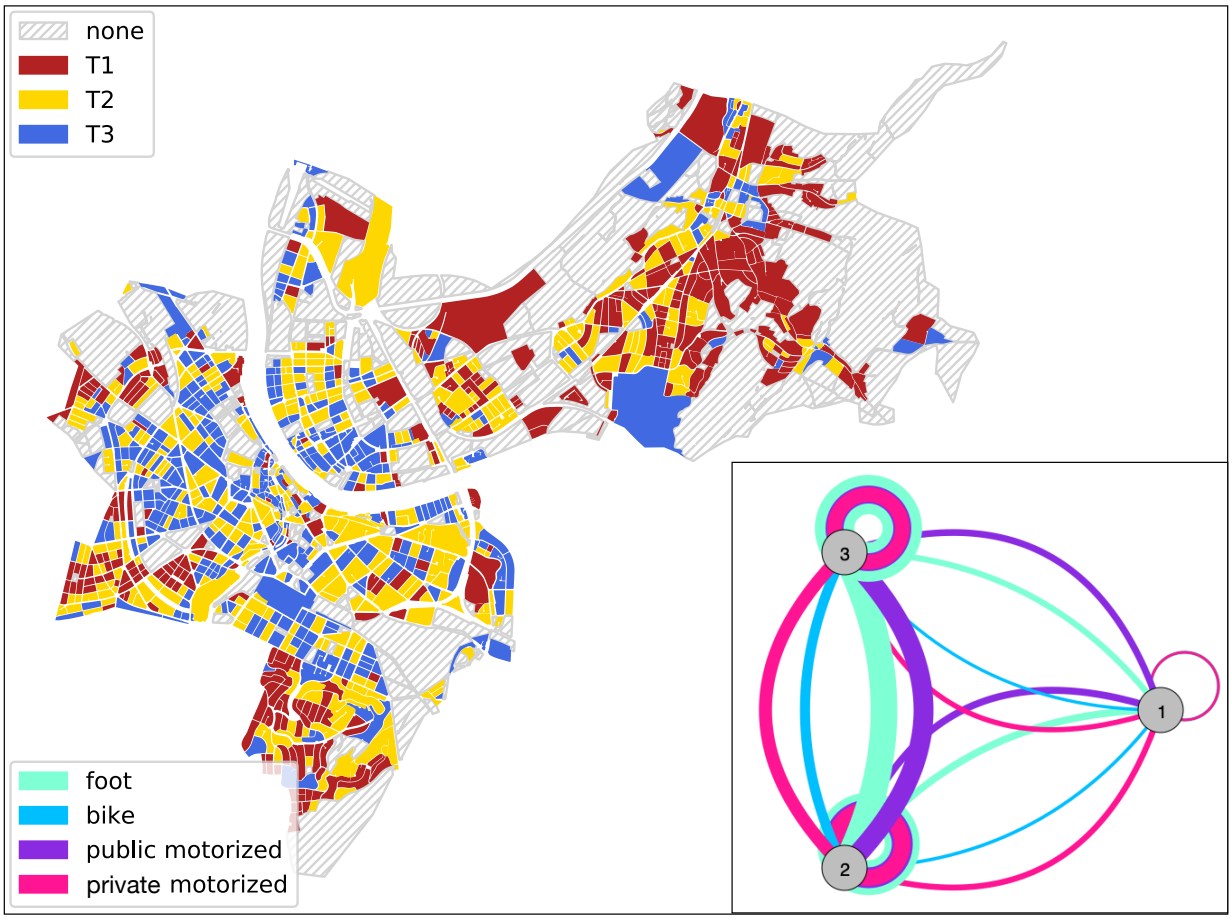

Figure S3: The Canton of Basel-City and its delineation with respect to statistical blocks colored according to the partition into tertiles T1, T2, and T3 of increasing fraction of 1-person households per block as provided by the canton's office for statistics. Inset: resulting mobility-graph, with nodes representing tertiles and edges representing effective connectedness through mobility by means of various modes of transport (thicker/thinner edges indicating weaker/stronger connectedness), as computed from the traffic-model provided by the traffic department of the Canton of Basel-City.

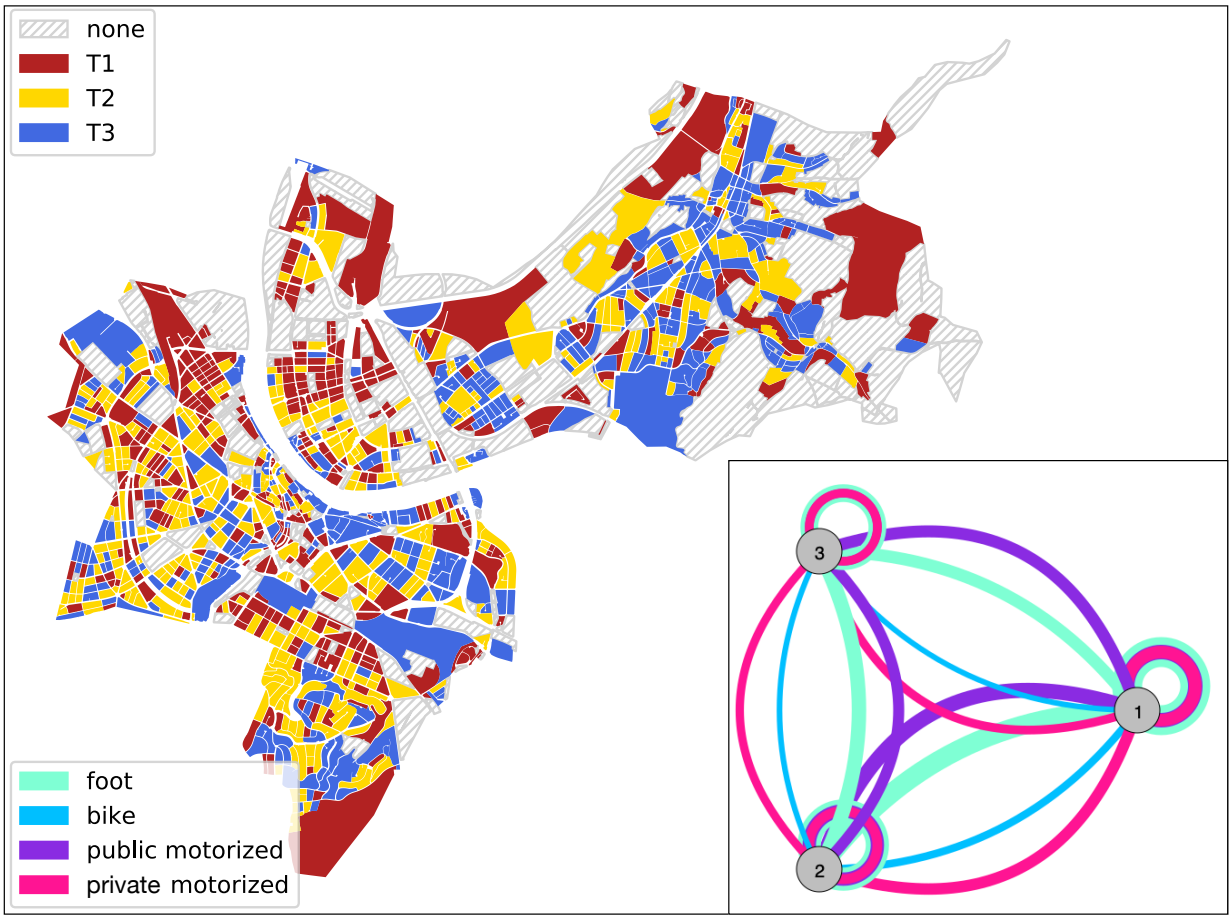

Figure S4: The Canton of Basel-City and its delineation with respect to statistical blocks colored according to the partition into tertiles T1, T2, and T3 of increasing fraction of residents aged older than 64 per block as provided by the canton's office for statistics. Inset: resulting mobility-graph, with nodes representing tertiles and edges representing effective connectedness through mobility by means of various modes of transport (thicker/thinner edges indicating weaker/stronger connectedness), as computed from the traffic-model provided by the traffic department of the Canton of Basel-City.

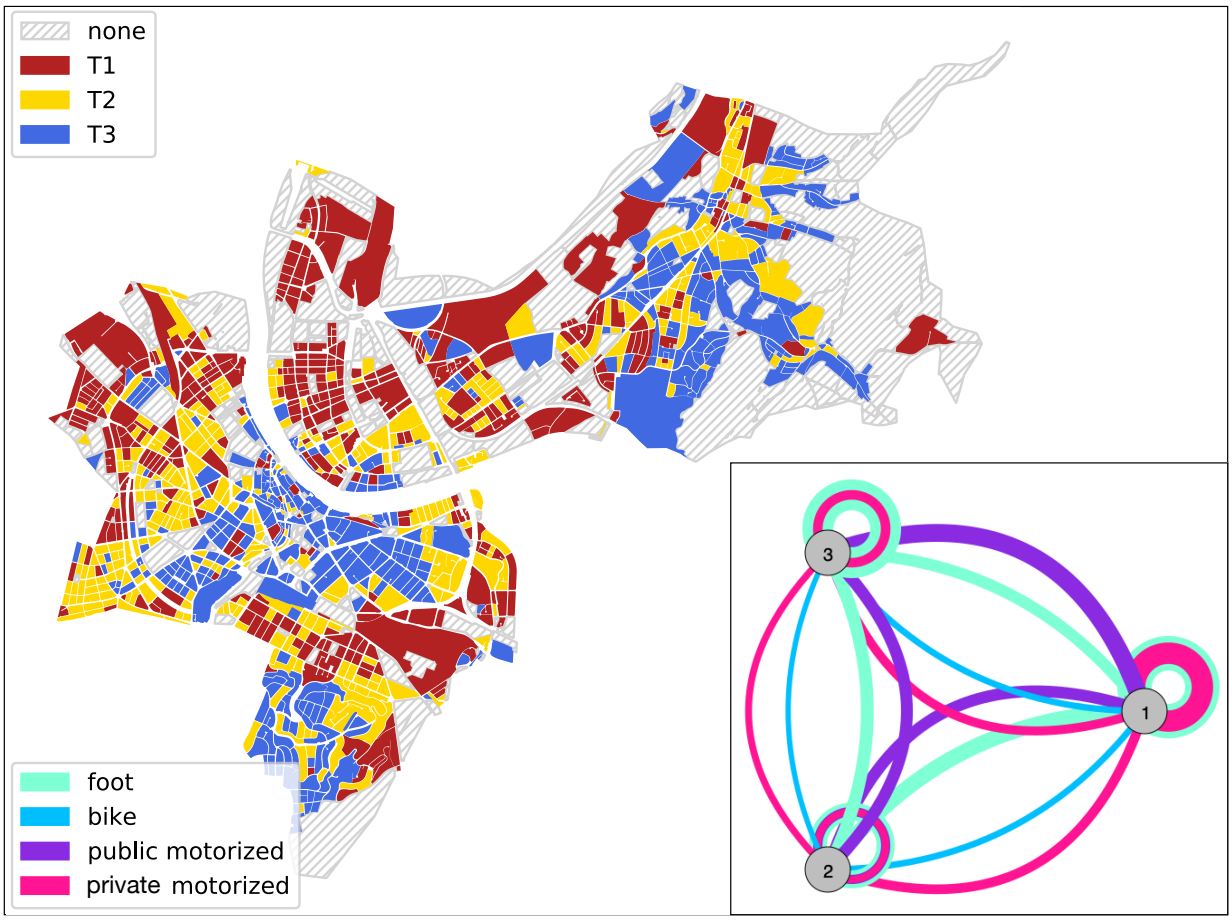

Figure S5: The Canton of Basel-City and its delineation with respect to statistical blocks colored according to the partition into tertiles T1, T2, and T3 of increasing living space per person as provided by the canton's office for statistics. Inset: resulting mobility-graph, with nodes representing tertiles and edges representing effective connectedness through mobility by means of various modes of transport (thicker/thinner edges indicating weaker/stronger connectedness), as computed from the traffic-model provided by the traffic department of the Canton of Basel-City.

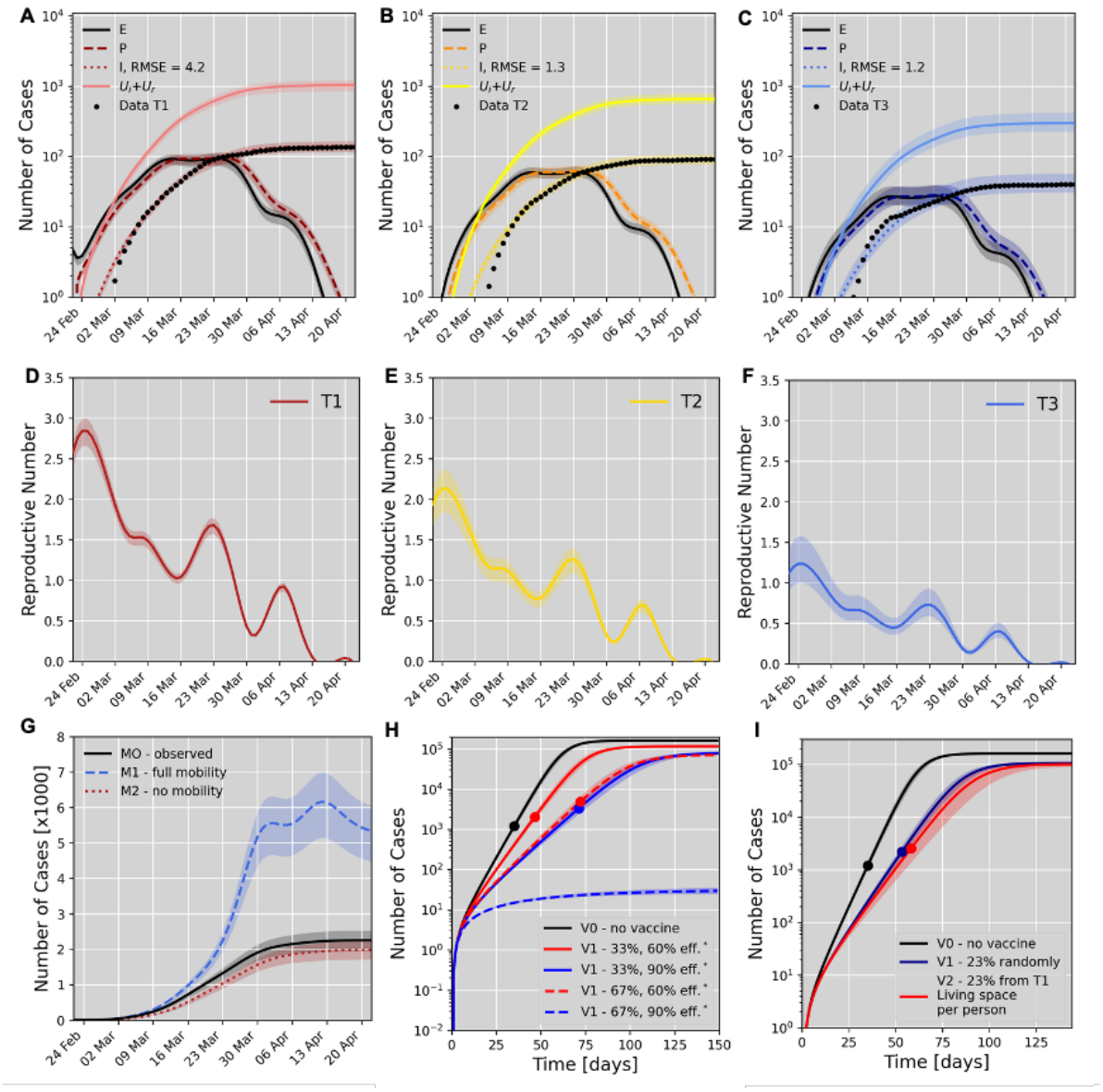

Figure S6: Data fit, reproductive number, and simulation of mobility and vaccination scenarios for a partition according to living space per person. A-C) Model fit to the case number time-series. Data points are shown together with model predictions based on undisturbed data (solid lines), and fifty bootstraps from disturbed data (bands) for the different tertitles T1(A), T2 (B) and T3 (C). D-F) The dynamic variation of the effective reproductive number for each of the tertiles shown in A-C). G) Influence of the mobility pattern on the total number of infected cases (sum of reported and unreported cases) assuming either no change in mobility (M1, 100% mobility), or full shut-down of all inner city mobility (M2, zero mobility). For comparison the observed scenario (M0) is shown. H) Prediction of vaccination effects if a specific percentage of all citizens was randomly selected for vaccination at given efficacy (scenario V1) compared to a simulation in the absence of any vaccination (V0). I) Prediction of vaccination effects if a specific percentage of all citizens was selected for vaccination from tertile T1 according to living space per person (scenario V2) together with the relevant scenarios V0 and V1. In H) and I) Simulations were performed assuming 90% vaccine efficacy for both SARS-CoV-2 transmission and prevention of severe COVID-19. Dots indicate the time of reaching 50% ICU occupancy.

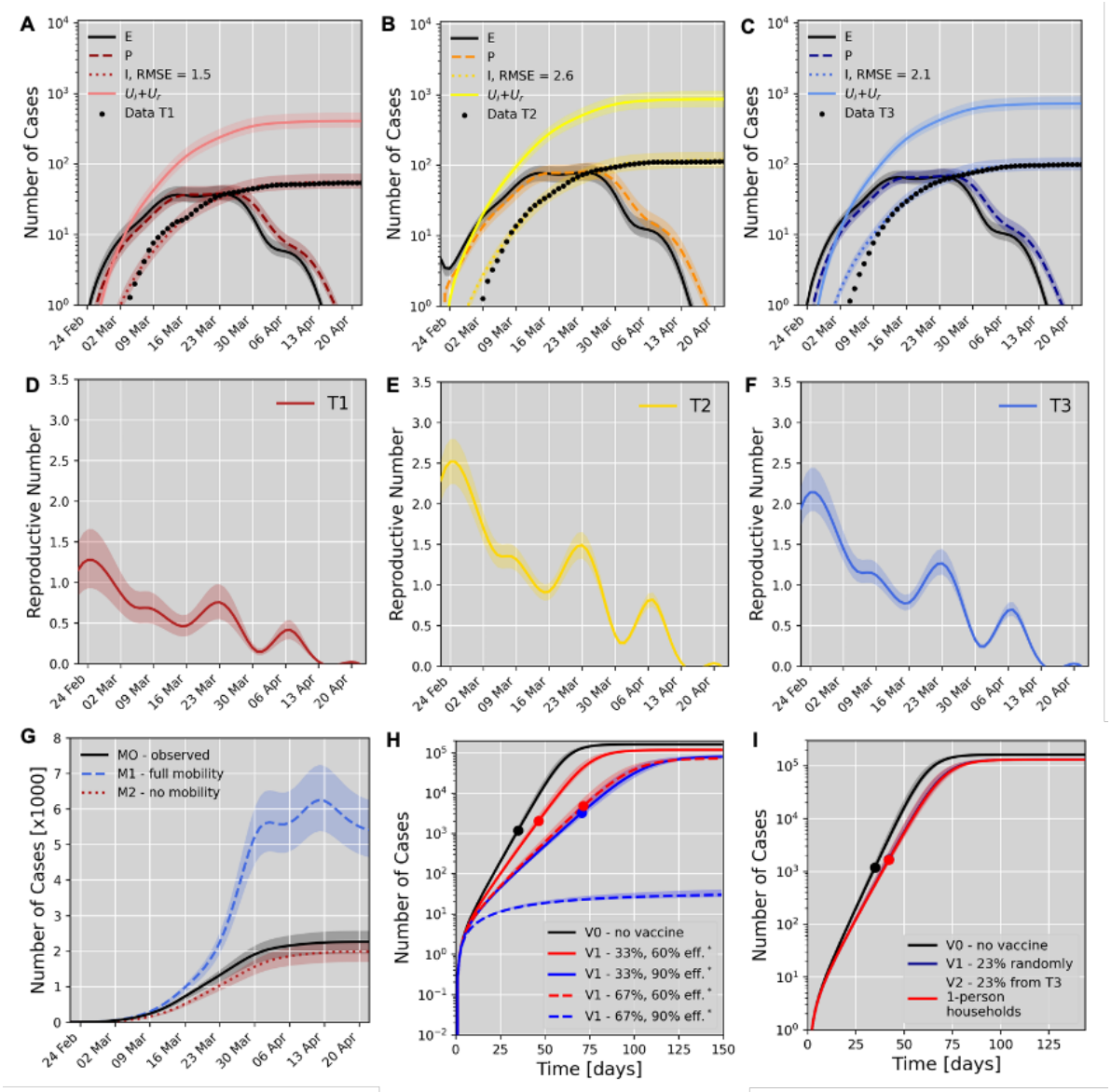

Figure S7: Data fit, reproductive number, and simulation of mobility and vaccination scenarios for a partition according to the share of 1-person households. A-C) Model fit to the case number time-series. Data points are shown together with model predictions based on undisturbed data (solid lines), and fifty bootstraps from disturbed data (bands) for the different tertitles T1(A), T2 (B) and T3 (C). D-F) The dynamic variation of the effective reproductive number for each of the tertiles shown in A-C). G) Influence of the mobility pattern on the total number of infected cases (sum of reported and unreported cases) assuming either no change in mobility (M1, 100% mobility), or full shut-down of all inner city mobility (M2, zero mobility). For comparison the observed scenario (M0) is shown. H) Prediction of vaccination effects if a specific percentage of all citizens was randomly selected for vaccination at given efficacy (scenario V1) compared to a simulation in the absence of any vaccination (V0). I) Prediction of vaccination effects if a specific percentage of all citizens was selected for vaccination from tertile T2 according to the share of 1-person households (scenario V2) together with the relevant scenarios V0 and V1. In H) and I) Simulations were performed assuming 90% vaccine efficacy for both SARS-CoV-2 transmission and prevention of severe COVID-19. Dots indicate the time of reaching 50% ICU occupancy.

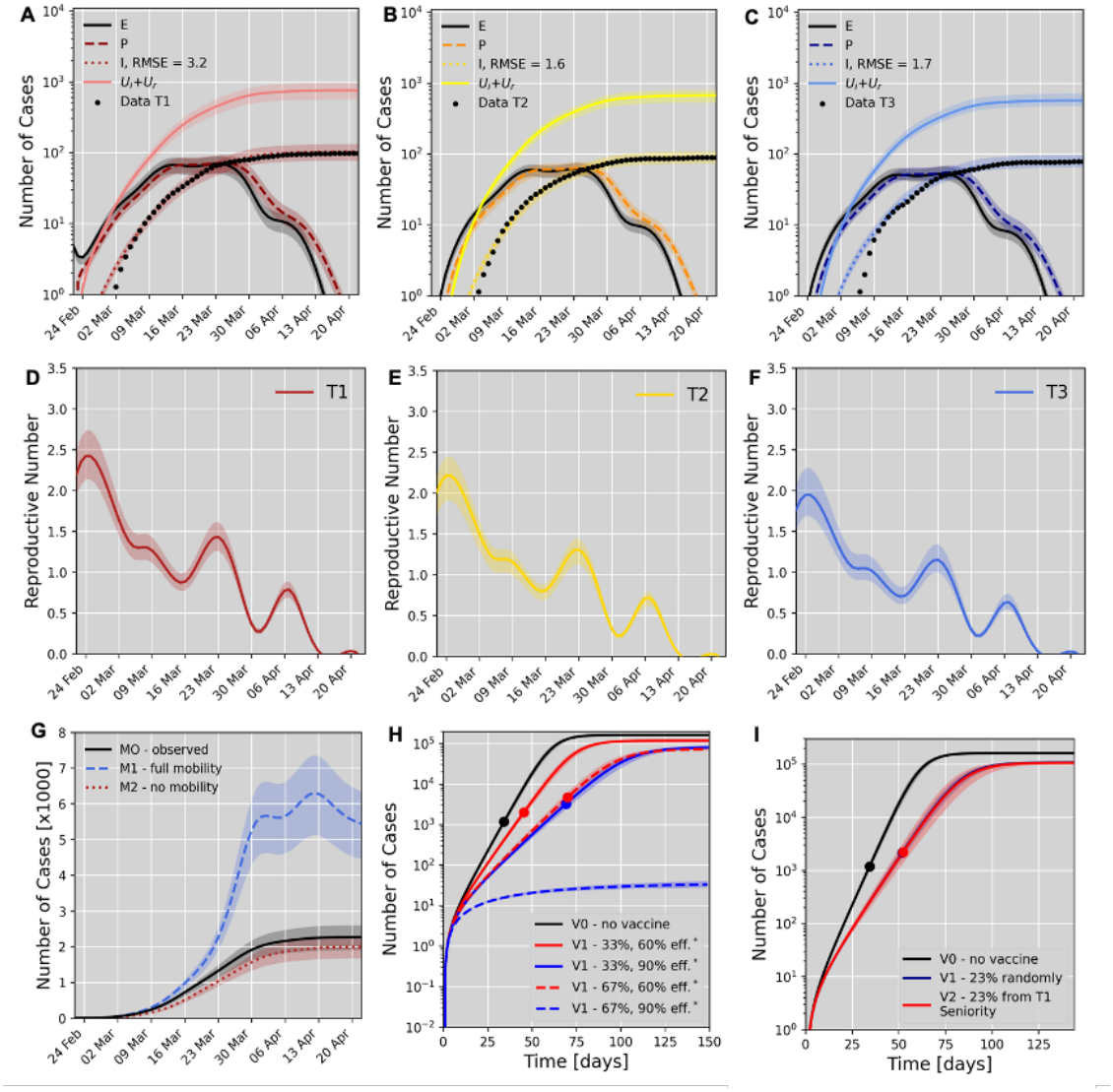

Figure S8: Data fit, reproductive number, and simulation of mobility and vaccination scenarios for a partition according to the share of senior residents. A-C) Model fit to the case number time-series. Data points are shown together with model predictions based on undisturbed data (solid lines), and fifty bootstraps from disturbed data (bands) for the different tertiles T1(A), T2 (B) and T3 (C). D-F) The dynamic variation of the effective reproductive number for each of the tertiles shown in A-C). G) Influence of the mobility pattern on the total number of infected cases (sum of reported and unreported cases) assuming either no change in mobility (M1, 100% mobility), or full shut-down of all inner city mobility (M2, zero mobility). For comparison the observed scenario (M0) is shown. H) Prediction of vaccination effects if a specific percentage of all citizens was randomly selected for vaccination at given efficacy (scenario V1) compared to a simulation in the absence of any vaccination (V0). I) Prediction of vaccination effects if a specific percentage of all citizens was selected for vaccination from tertile T1 according to the share of senior residents (scenario V2) together with the relevant scenarios V0 and V1. In H) and I) Simulations were performed assuming 90% vaccine efficacy for both SARS-CoV-2 transmission and prevention of severe COVID-19. Dots indicate the time of reaching 50% ICU occupancy.

Urban quarters in Basel-City.

Figure S9: Urban quarters in Basel-City.

A Table.Number of phylogentic clusters in Basel-City quarters within lineage B.1-C15324T (N = 70) and among all intodruced lineages (N = 128). Please note that clusters can be shared among quarters and therefore to not add up to N.

	N clusters in B.1-C15324T	N clusters in Basel-City	N infected persons in B.1-C15324T	N infected persons Basel-City
Oldtown Grossbasel	0	1	0	1
Oldtown Kleinbasel	1	3	1	3
Am Ring	11	19	25	34
Bachletten	15	22	22	34
Breite	6	10	7	13
Bruderholz	6	7	12	15
Clara	2	6	2	7
Gotthelf	8	12	9	15
Gundeldingen	13	25	18	41
Hirzbrunnen	5	9	5	9
Iselin	12	19	19	28
Kleinhüningen	4	5	7	11
Klybeck	8	8	11	11
Matthäus	12	22	19	33
Riehen	15	18	28	35
Rosental	3	11	4	15
St. Alban	6	9	11	19
St. Johann	14	27	23	42
Vorstädte	5	9	6	14
Wettstein	6	6	8	8
w/o adress	8	11	10	23

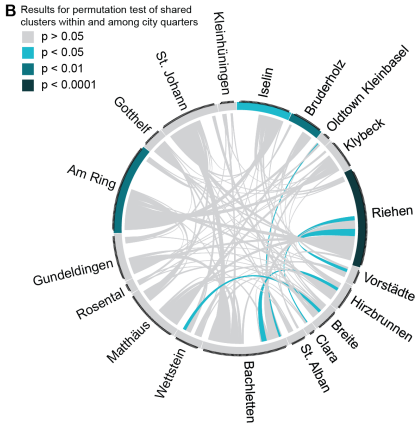

Figure S10: Phylogenetic clusters in quarters of Basel-City. A) Number of clusters within B.1-C15324T and within all viral variants in quarters of Basel-City. B) Visualisation of permutation analysis of shared phylogenetic clusters within and among urban quarters in Basel-City.

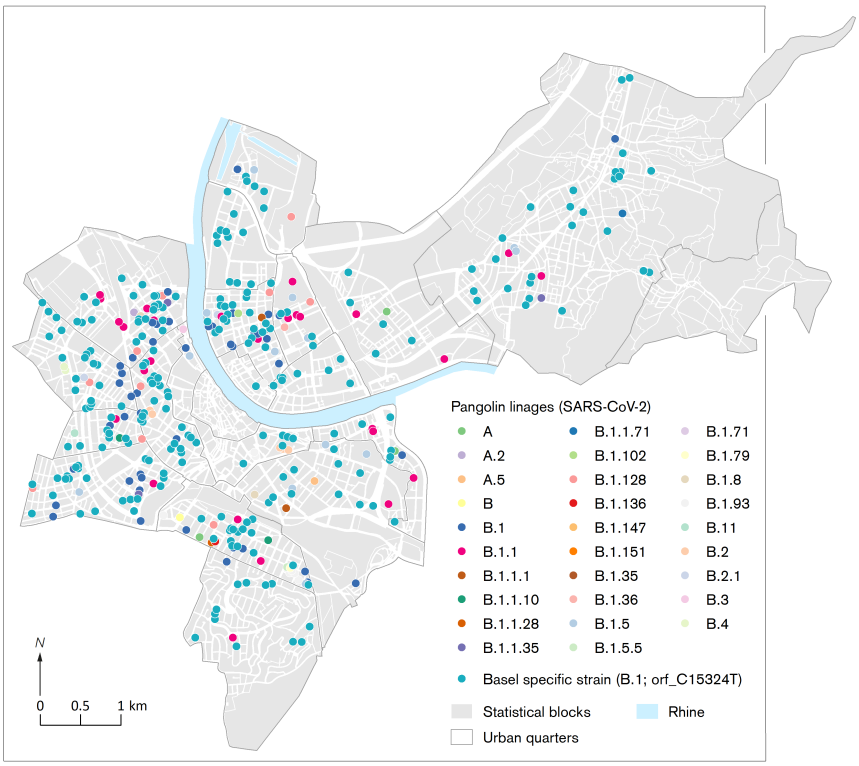

Figure S11: Lineage identity (pangolin) of PCR-confirmed COVID-19 cases from 26th of February until 22nd of April, 2020, in Basel-City with B.1-C15324T as dominant variant highlighted.

socioeconomic indicator	achieved significance level
living space per person	1%
median income	2%
fraction of 1-person households	2%
fraction of residents aged above 64	45%

Table S2: Achieved significance level (ALS) of maximum differences in R_{eff} associated with a partition of housing blocks according to various socioeconomic indicators. ALSs have been obtained by comparing these differences in R_{eff} with those obtained from 99 bootstrapping random partitions.

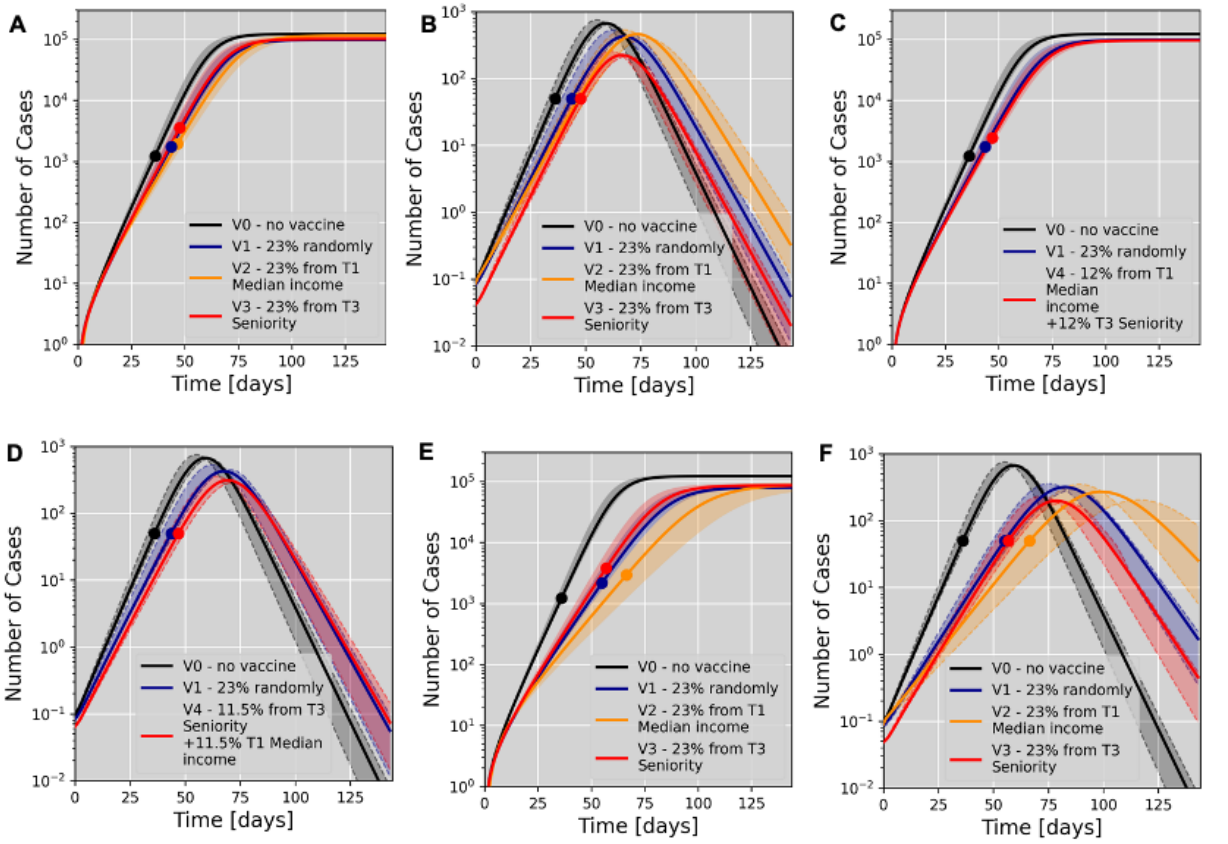

Figure S12: Modelling of vaccine scenarios assuming 60% (A-D) or 90% (E, F) vaccine efficacy to prevent SARS-CoV-2 transmission and 90% (A-D) or 70% (E, F) efficacy against severe COVID-19. We compare with scenarios V0 (no vaccination) and V1 (vaccination at random). Dots indicate the time of reaching a 50% ICU occupancy. A) Simulation of vaccination effects based on a partition according to median income. Scenario V2 models vaccination of 23% of all citizens selected from the tertile with the lowest median income (T1). Scenario V3 models vaccination of 23% of all citizens selected from the tertile with the highest share of senior residents (T3). B) Temporal evolution of ICU occupancy for the scenarios modelled in A). C) Simulation of a mixed vaccination strategy giving equal priority to senior citizens and mobile population groups. D) Temporal evolution of ICU occupancy for the scenarios modelled in C). E) Simulation of the same scenarios as in A) assuming 70% effective vaccination against severe COVID-19, and 90% vaccine efficacy to prevent SARS-CoV-2 transmission. F) Temporal evolution of ICU occupancy for the scenarios modelled in E).

1. Leuzinger, K. *et al.* Epidemiology of Severe Acute Respiratory Syndrome Coronavirus 2 Emergence Amidst Community-Acquired Respiratory Viruses. *The Journal of infectious diseases* (2020). URL http://www.ncbi.nlm.nih.gov/pubmed/33180912.

2. Kanton Basel-Stadt Datenportal (data.bs.ch 2021). Coronavirus (COVID-19): Fallzahlen Basel-Stadt (2021). URL https://data.bs.ch/explore/dataset/100073.

3. Stange, M. *et al.* SARS-CoV-2 outbreak in a tri-national urban area is dominated by a B.1 lineage variant linked to a mass gathering event. *medRxiv; accepted for publication in PLOS Pathogens* 2020.09.01.20186155 (2021). URL https://doi.org/10.1101/2020.09.01.20186155.

4. Statistisches Amt Basel-Stadt: Bevölkerungsstatistik. Statistisches Jahrbuch des Kantons Basel-Stadt: Wohnbevölkerung nach Geburtsjahr, Heimat und Geschlecht [t01.1.14] (2021).

5. Elbe, S. & Buckland-Merrett, G. Data, disease and diplomacy: GISAID's innovative contribution to global health. *Global Challenges* **1**, 33–46 (2017). URL https://pubmed.ncbi.nlm.nih.gov/31565258/.

6. Shu, Y. & McCauley, J. GISAID: Global initiative on sharing all influenza data – from vision to reality. *Eurosurveillance* **22**, 2–4 (2017). URL https://www.eurosurveillance.org/content/10.2807/1560-7917.ES.2017.22.13.

7. Hadfield, J. *et al.* NextStrain: Real-time tracking of pathogen evolution. *Bioinformatics* **34**, 4121–4123 (2018). URL https://pubmed.ncbi.nlm.nih.gov/29790939/.

8. Huerta-Cepas, J., Serra, F. & Bork, P. ETE 3: Reconstruction, Analysis, and Visualization of Phylogenomic Data. *Molecular Biology and Evolution* **33**, 1635–1638 (2016). URL https://academic.oup.com/mbe/article/33/6/1635/2579822.

9. Ragonnet-Cronin, M. *et al.* Automated analysis of phylogenetic clusters. *BMC Bioinformatics* **14**, 317 (2013).

10. Egli, A. *et al.* High-resolution influenza mapping of a city reveals socioeconomic determinants of transmission within and between urban quarters. *bioRxiv* (2020). URL https://www.biorxiv.org/content/early/2020/04/04/2020.04.03.023135. https://www.biorxiv.org/content/early/2020/04/04/2020.04.03.023135.full.p

11. Krzywinski, M. *et al.* Circos: an information aesthetic for comparative genomics. *Genome research* **19**, 1639–45 (2009). URL http://www.ncbi.nlm.nih.gov/pubmed/19541911 http://www.pubmedcentral.nih.gov/articlerender.fcgi?artid=PMC2752132.

12. Bau- und Verkehrsdepartement Basel-Stadt Mobilität / Mobilitätsstrategie. Gesamtverkehrsmodell der Region Basel, Basismodell: “Ist-Zustand 2016” (2020).

13. Kalman, R. E. *et al.* Contributions to the theory of optimal control. *Bol. soc. mat. mexicana* **5**, 102–119 (1960).

14. Welch, G., Bishop, G. *et al.* An introduction to the kalman filter (1995).

15. AstraZeneca. AZD1222 vaccine met primary efficacy endpoint in preventing COVID-19 (2020).

16. Mahase, E. Covid-19: Moderna vaccine is nearly 95% effective, trial involving high risk and elderly people shows. *BMJ: British Medical Journal (Online)* **371** (2020).

17. Canton Basel-City, Department of Presidential Affairs, External Affairs and Marketing 2021: Regional, national and trinational cooperation. URL: https://www.marketing.bs.ch/en/institutional-cooperation/tri-national-cooperation.html .

18. TEB-Trinationaler Eurodistrict Basel 2021:https://www.eurodistrictbasel.eu/de/home.html.

19. European Commission Eurostat: Metropolitan regions. URL : https://ec.europa.eu/eurostat/web/metropolitan-regions/background.

20. Dijkstra, L., Poelman, H. & Veneri, P. The EU-OECD definition of a functional urban area. OECD Regional Development Working Papers 2019/11, OECD Publishing (2019). URL `https://ideas.repec.org/p/oec/govaab/2019-11-en.html`.

21. EURES-T Oberrhein 2021: https://www.eures-t-oberrhein.eu/.

22. Canton Basel-City Statitsics Office: Cross-border commuters 2020, based on Federal Statistics Office Cross-border statistics Indicator I.03.5.2152. https://www.statistik.bs.ch/haeufig-gefragt/arbeiten/grenzgaenger.html.

23. Perkmann, M. Cross-Border Regions in Europe. *European Urban and Regional Studies* **10**, 153–171 (2003). URL http://journals.sagepub.com/doi/10.1177/0969776403010002004.

24. EURES-T Oberrhein 2021: https://www.aebr.eu/.

25. Randstadt Region 2019 Randstad Monitor 2019. https://www.nl-prov.eu/wp-content/uploads/2019/05/randstad-monitor-gecomprimeerd-2-gecomprimeerd-compressed.pdf.

26. Randstadt Region 2017 Randstad Monitor 2017. https://www.nl-prov.eu/wp-content/uploads/2017/11/regio-randstad-monitor-2017.pdf .

27. Trinationale Metropolregion Oberrhein 2021. Wirtschaft. https://www.rmtmo.eu/de/wirtschaft.html .

28. Trinationale Metropolregion Oberrhein 2021. Metropolregion. https://www.rmtmo.eu/de/metropolregion.html.

29. Jay, J. *et al.* Neighbourhood income and physical distancing during the COVID-19 pandemic in the United States. *Nature human behaviour* (2020). URL http://www.ncbi.nlm.nih.gov/pubmed/33144713.

30. De Ridder, D. *et al.* Socioeconomically Disadvantaged Neighborhoods Face Increased Persistence of SARS-CoV-2 Clusters. *Frontiers in Public Health* **8** (2021). URL https://www.frontiersin.org/articles/10.3389/fpubh.2020.626090/full.

31. Bluhm, A. *et al.* SARS-CoV-2 transmission routes from genetic data: A Danish case study. *PLOS ONE* **15**, e0241405 (2020). URL https://dx.plos.org/10.1371/journal.pone.0241405.